Chapter 1

Introduction

CHAPTER 1: Introduction

1.1 Global Energy Demand

The global energy requirement is increasing rapidly in order to meet the need of population growth and technological advancements. With the increase in population and technological advancement, the electricity demand is increasing day by day. Electricity is an essential part of modern life and it helps us in many ways, such as heating, lighting, cooling, medical purposes, operating equipments, public transportation systems, electronics, etc. Electricity reduces the isolation of rural areas from other areas. Moreover, safety is also achieved by providing external lighting, alarm systems, and even traffic lights, as electricity is necessary to facilitate human life for safety in homes, cities, and major areas. Electricity can be produced by converting basic and natural energy sources such as coal, solar energy, natural gas, wind power, and nuclear power into electrical energy.

When we look at global energy demand, we can break it into five categories: nuclear, oil, coal, natural gas, and renewable energy. Conventional energy resources (eg, oil, gas, and coal) contributed greatly to global electricity generation. As shown in Figure 1.1(a), global energy use is heavily dependent on fossil fuels such as coal, natural gas, and oil. As an example, non-renewable energy sources such as fossil fuels (oil, coal, and natural gas), nuclear energy currently meet more than half of the world's total energy demand. These conventional sources are small and they suffer from several drawbacks associated with their use, such as emissions, limited reverse, and price increases. They have also contributed to the increase in pollution globally and the deterioration of human health. Hydroelectric power, wind, and solar

(renewable sources) are the fastest-growing energy sources between 2018 and 2050, with rapid growth in electricity generation. It has become the most widely used energy source, leaving behind petroleum and other liquids (shown in Fig. 1.1 (a)). Worldwide renewable energy consumption grew by 3.1% per year between 2018 and 2050, compared to a 0.6% annual increase in petroleum and other liquids, a 0.4% increase in coal, and a 1.1% annual increase in natural gas consumption. To meet the global energy demand, the consumption of fossil fuels has to be reduced. Conversely, the use of renewable energy sources like solar panels, wind turbines, etc should be increased. Consequently, for the long-term sustainability of society, it is vital to convert to renewable energy sources. Therefore, we need an energy source that is more energy-efficient, does not harm the environment, and is also commercially viable [1]. Many research activities are being executed to achieve an efficient power generation system. Since the traditional technology of burning fossil fuels cannot meet the increased need for electricity, however hydro, solar and wind, can act as custodians in an energy crisis [2]. Solar energy is the most abundant alternative energy source available among all energy sources. Since India is a fast-growing economic country, energy consumption is also increasing sharply (shown in Fig 1.1(b)) [3]. Keeping this in mind, the government of India has made an ambitious plan with an energy target of 175 Gigawatt (GW) by 2022, which includes solar power (100 GW) and wind power (60 GW) [4]. In addition, this target has been increased to 227 Gigawatt (till 2027) [5]. Fig. 1.1(a) depicts the historical and expected global energy consumption by different sectors up to the year 2050 of world energy consumption which is based on the study. Further, the total energy consumption in selected countries and regions from 1990-2050 (as shown in Fig. 1.1(b), International Energy Outlook 2019).

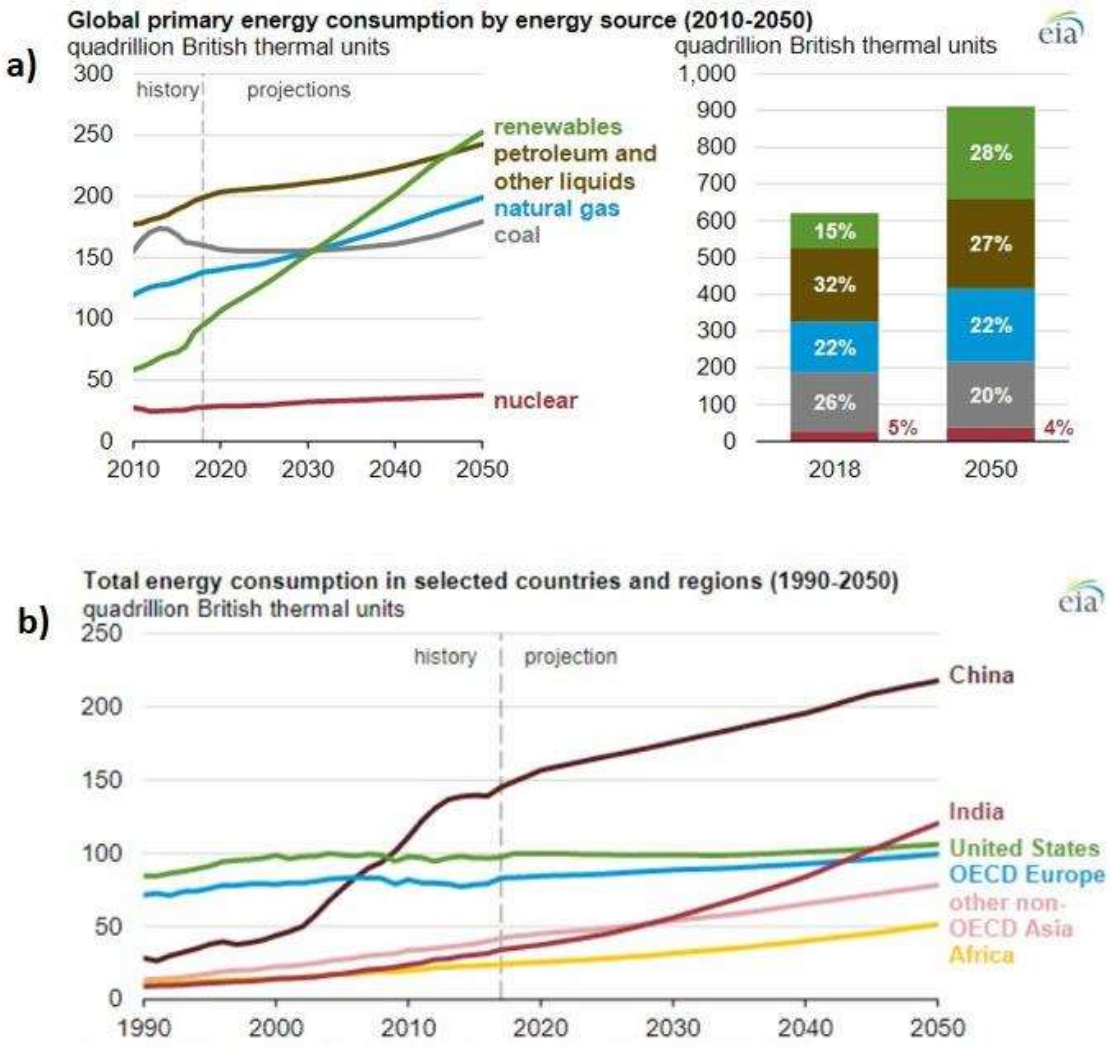

Figure 1.1: (a) Energy consumption by energy sources from 2010 to 2050. (b) Represents the total energy consumption in selected countries and regions from 1990-2050 (Ref: en.wikipedia.org.).

1.2 Solar Energy

Solar energy is radiant light and heat from the Sun, often called solar resource or sunlight, is electromagnetic radiation emitted by the Sun. The sun is a unique and renewable resource that can fuel life on earth and provide sustainable energy, clean to all of its inhabitants. Thus, solar energy along with a clean and sustainable energy source provides significant benefits to

both the climate and economy of both developed and developing countries in the times to come [6]. About 29 percent of the incoming radiation is received at the top of the atmosphere and reflected back into space by atmospheric particles, clouds, or shiny ground surfaces such as sea ice and snow. This energy has no role in Earth's climate system. The atmosphere absorbs about 23 percent of it from dust, ozone, and water vapor while the surface absorbs 48 percent which passes through the atmosphere. In this way, 71% of incoming solar energy is received by the Earth system [7], [8]. Solar radiation arises from the photosphere of the Sun and has an outer temperature of about 5800 K (shown in Fig. 1.2). The Spectrum resembles a black body radiator at the same temperature [9].

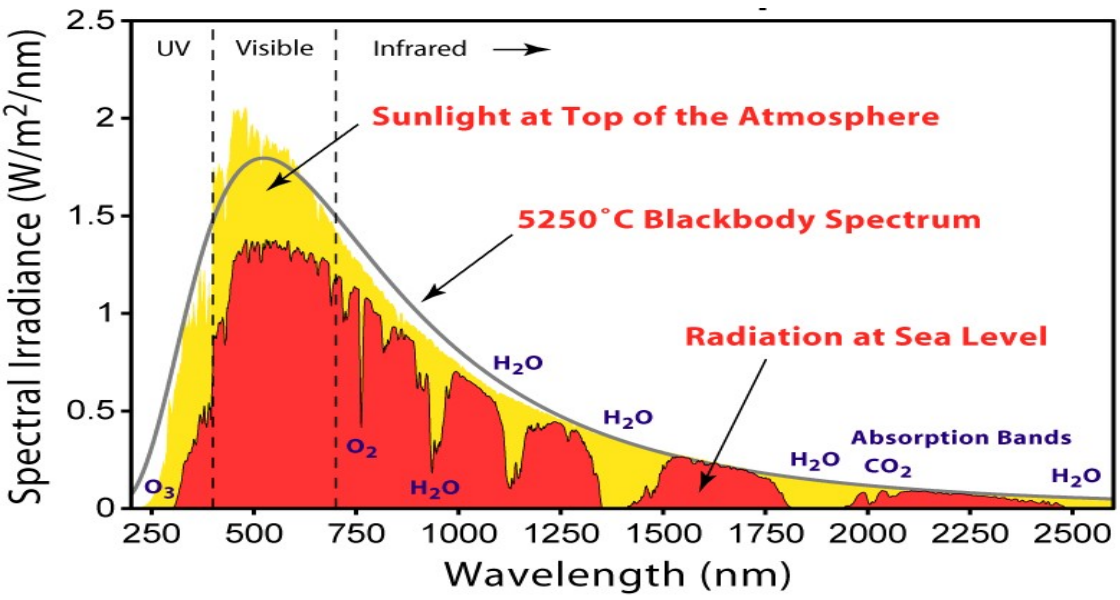

Figure 1.2: Depicts the solar radiation spectrum (Ref: en.wikipedia.org.).

The surface of the Earth absorbs the sunlight, wavelength range from ultraviolet to infrared. A solar thermal system and a solar photovoltaic (PV) system are today's two main types of solar energy technology. The first is a solar-thermal system that uses the mirror to

reflect and focus sunlight onto receivers and collect solar energy to convert it into heat. It is mainly used in very large power plants. Second is the solar photovoltaic (PV) system in which light strikes the solar panel and converts it into electricity. Thus photovoltaic (photo = light, voltaic = electricity) solar cells to generate electricity appear as a promising way to convert sunlight into electricity.

1.3 Solar Cells: An Overview

Photovoltaics is the phenomenon that converts sunlight into electricity using semiconductor materials and this effect is called the photovoltaic effect [10]. *Edmund Becquerel* has first discovered the photovoltaic effect in 1839. He observed that the exposure to light on a silver (Ag) coated platinum (Pt) electrode immersed in the electrolyte-generated electric current [11].

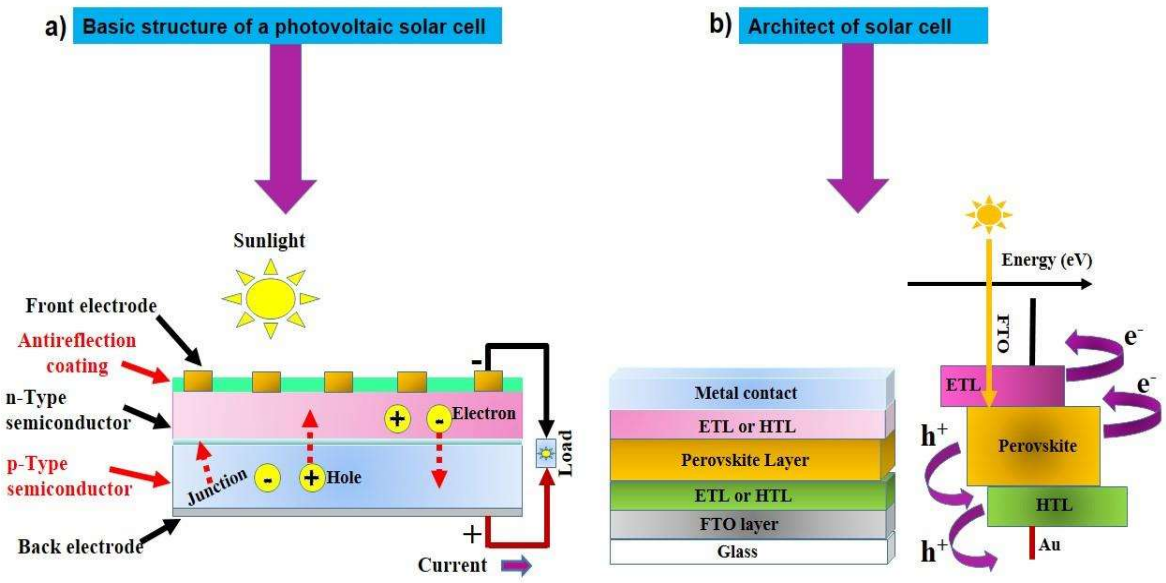

Figure 1.3: (a) Depicts the structure of a solar cell and (b) represents an architect of a solar cell.

A photovoltaic solar cell is made of three main parts [12]. First is the light absorber (converts incident photons to holes and electrons). The second is the carrier collectors (capturing the electrons and holes) and the third is the metal contacts (transferring the carriers to the circuit). Fig. 1.3(b) is showing the architecture of solar cells with different layers. When sunlight falls on the perovskite layer (act as an active layer, photon absorption in perovskite layer), electrons and holes are produced from this layer. The photogenerated electrons move towards the cathode through the electron transport layer (ETL) and the holes move towards the anode through-hole transport layer (HTL). The role of ETL and HTL is to assemble the photogenerated charge carriers and facilitate their transport to the respective electrodes [13].

Following are the four processes by which we can understand the operation of solar cells in detail [14],[15]: First is the absorption of incident photons. Second is the generation of photo-generated charge carriers (electron-hole pairs). The third is the transportation of these photogenerated charge carriers and the fourth is the collection of charge carriers into an external circuit.

1.3.1 The absorption of incident photons

The absorption of incident photons is the first step in functioning a solar cell. It primarily depends on the energy levels of the absorber layer and the energy of each incident photon. A semiconductor material is used as an active layer (absorber layer) material in solar cells which are semiconductor materials based on bandgap (the energy gap between the valence band (VB) and the conduction band (CB)). Here, the valence band is the highest energy band occupied by electrons, and the conduction band is the lowest energy band where there is no state. When a photon is incident on material whose energy is greater than equal to the bandgap, excites an

electron from VB to CB. In this process, an excess amount of energy is lost through thermalization. Furthermore, if the photon's energy is less than the bandgap energy, it will not be absorbed by the material but transmitted [16].

1.3.2 The generation of photo-generated charge carriers (electron-hole pairs)

In the second step, photon absorption creates an excited electron (negatively charged, e-) in the CB and an electron vacancy in the VB known as hole (positively charged, h+). These electron-hole pairs can be thought of as free charges mostly in the inorganic semiconductors at room temperature. The Coulomb interaction strongly binds together the electron-hole pairs. The interaction contributes to the stabilizing energy balance and the electron-hole pair forms an exciton. For the photovoltaic effect to occur, the exciton needs some additional energy to create free electrons and holes to move freely through the active material [14].

1.3.3 The transportation of these photogenerated charge carriers

The separation and collection of free-charge carriers are the next steps of solar cell operation. Diffusion-based transport and drift-based transport are two transport mechanisms that contribute to this procedure. In a diffusion-based transport mechanism, the transport of charge carriers in semiconductor materials is caused by a concentration gradient, whereas, in a drift-based transport mechanism, the transport of charge carriers is generated by an electric field. Therefore, these two mechanisms will play a decisive role in transporting free charge carriers through the active material.

1.3.4 The collection of photo-generated charge carriers

The collection of photo-generated charge carriers (electrons and holes) at the electrode into the external circuit is the final stage of solar cell operation. An ohmic contact collects the charge carriers between the electrode and the semiconductor. The work function of the electrode should be lower than the work function of the semiconductor to prevent the Schottky barrier for the collection of electrons. Further, the work function of the electrode should be higher than the semiconductor's work function for hole collection. A cycle has been completed when an electron reaches the electrode, dissipates the energy, and produces the power. After that, it recombines with the hole on the opposite electrode. Hence, appropriate selections of electrode material and the proper transport layers are essential to achieve the high-power conversion efficiency (PCE) of solar cells.

1.4 Characteristics of Solar Cells

Solar cell performance can be understood as the parameters of solar cells exposed to sunlight that can be obtained from the I–V curve. Short circuit current (I_{SC}), Fill factor (FF), Open-circuit voltage (V_{oc}), power conversion efficiency (PCE), and maximum power output (P_{max}), are the essential parameters. Fig. 1.4 shows the solar cell equivalent circuit model. The ideal case of a solar cell, ($R_{sh} = \infty$) and ($R_s = 0$) are the shunt and series resistance, respectively. Here, I_D, I_L, and I_{SH} are the voltage-dependent current lost to recombination, light generated current in the cell, and the current loss due to the shunt resistance, respectively [17].

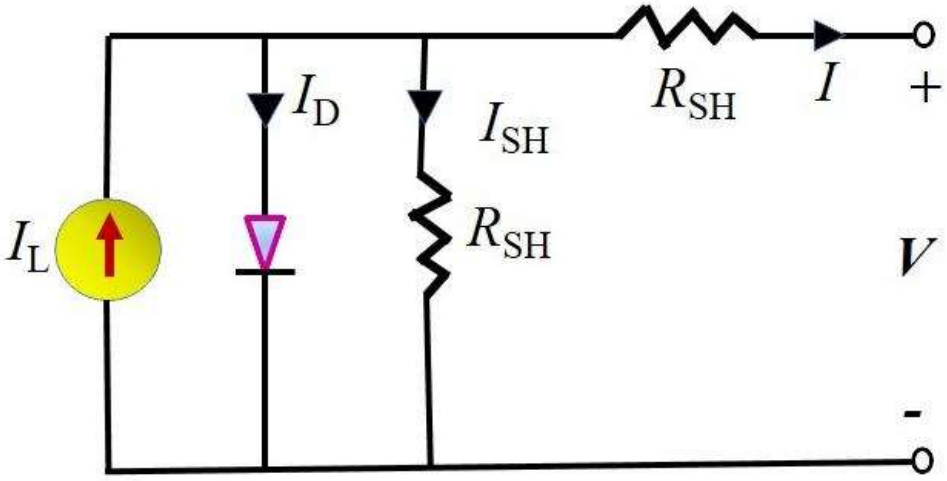

Figure 1.4: Represents the solar cell equivalent circuit model.

1.4.1 The I-V (Current-Voltage) Characteristics

The solar cell gives an I-V curve equivalent to that of a diode in the dark. The current-voltage curve of an ideal solar cell lies in the fourth quadrant. When light is incident on the solar cell, the I-V curve shifts in the 4th quadrant as the cell begins to generate electricity, the greater the intensity of the light on the cell, the greater the amount of shift. The equation of the current-voltage curve (fourth quadrant) is represented by:

$$I = I_L - I_0 \left[\exp\left(\frac{qV}{nkT}\right) - 1\right] \quad (1.1)$$

Where I_0, I_L, V, q, are the reverse saturation current of diode, photo-generated current, the applied voltage, and elementary charge, respectively. in addition to it, k, T, and n represent the Boltzman constant, temperature, and the ideality factor of a diode, respectively [18].

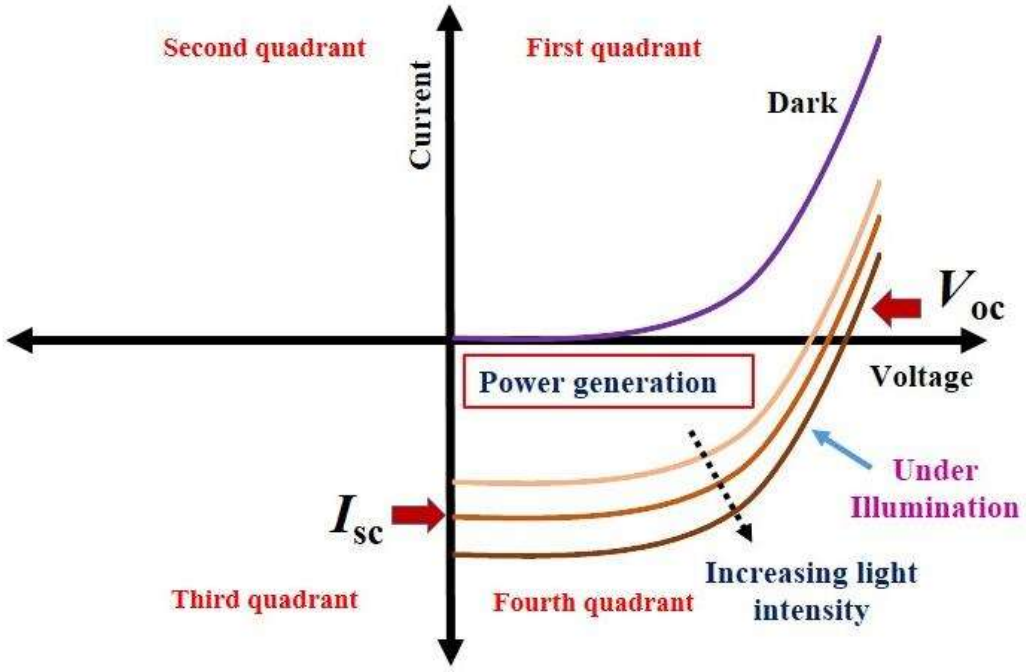

Figure 1.5: Schematic diagram of I-V peculiarities of a solar cell in dark and light.

1.4.2 Open-Circuit Voltage

It is the maximum possible voltage produced across the terminals of the solar cell when they are disconnected (shown in Fig. 1.6 (a)), i.e., the current is zero ($I = 0$). The open-circuit voltage can be seen on the I–V curve above (shown in Fig. 1.5). The V_{oc} equation is obtained by substituting the value of current ($I=0$) in the above solar cell equation (1.1).

$$V_{oc} = [\frac{nkT}{q}\ln(\frac{I_L}{I_0} + 1)] \quad (1.2)$$

V_{oc} depends on the I_0 (saturation current) and I_L (light-generated current) of the solar cell. While there is usually little variation in the I_{sc}, the main effect is I_0, as it may change by an order of magnitude. The Saturation current depends on the recombination in the solar cell. Thus, the amount of recombination in the device is measured by V_{oc}. In addition, V_{oc} is affected

by the morphology of the active layer material, so a better match between the semiconductor (deposited active layer) and the metal electrode is needed [19].

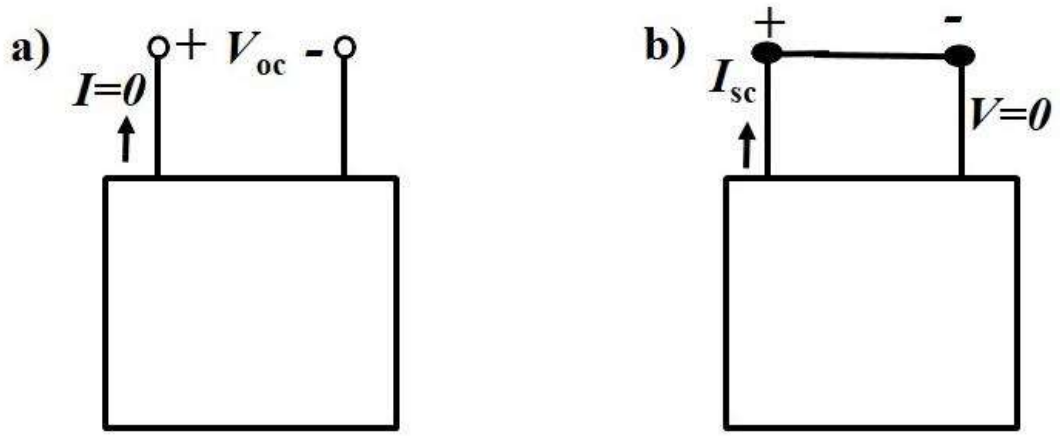

Figure 1.6: (a) Represents the open-circuit voltage and (b) shows the short-circuit current equivalent circuits.

1.4.3 Short-Curcuit Current (I_{sc})

I_{sc} is the maximum amount of current that flows through an external circuit when the electrodes of a solar cell are short-circuited. Thus, the cell will be short-circuited in this condition when V is zero (shown in Fig 1.6(b)). I_{sc} depends on the generation and collection of photo-generated charge carriers.

I_{sc} contains some dependency on electrical and optical factors such as solar cell area, light intensity, absorption and reflection coefficient, incident light's spectrum, active layer thickness, and collection efficiency. Surface passivation and diffusion length are important factors to differentiate solar cells made of similar materials. The short circuit current of an ideal cell with uniform generation and a passive surface is calculated as follows:

$$I_{sc} = qAG(L_n + L_p) \tag{1.3}$$

where G, A, L_n, L_p are the generation rate, an area of the solar cell, the diffusion length of electrons and holes, respectively. I_{sc} represents the strong proportionality of generation rate and diffusion length.

1.4.4 Maximum Power Output (P_{max})

Maximum power output is the maximum amount of power provided by a solar cell. It can be written as $P_{max} = I_m V_m$ where V_m is the maximum voltage and I_m is the maximum current. This can be seen in the current-voltage curve (Fig. 1.7). The operating point of the solar cell is the point at which the delivered power gains its maximum value.

1.4.5 Fill Factor (FF)

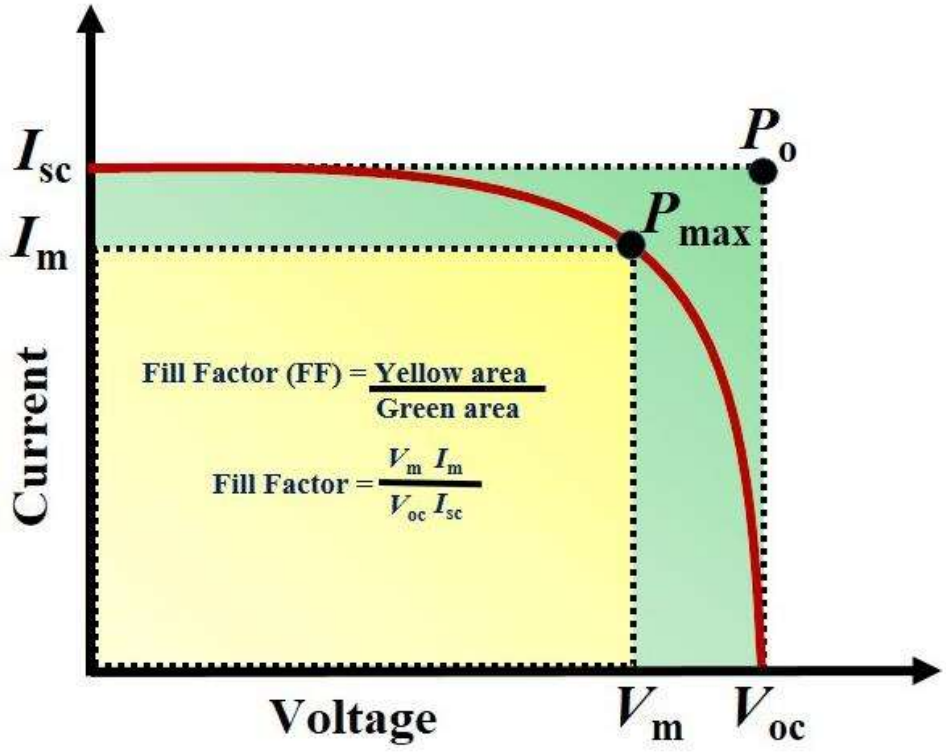

Figure 1.7: Schematic diagram of Fill Factor (FF) for a solar cell.

The performance of the solar cell can be understood by the FF and it is the ratio of P_{max} = V_m I_m that can be observed from a solar cell to P_o= V_{oc} I_{sc} (ideal power).

$$FF = \frac{V_m I_m}{V_{oc} I_{sc}} = \frac{P_{max}}{V_{oc} I_{sc}} \quad (1.4)$$

If for an ideal solar cell all the incident radiation is converted into electrical energy then the FF must be unity. However, the fill factor (FF) value for perovskite solar cells is in the range of 0.1 – 0.8 due to the presence of several disadvantages in the cell architecture. Moreover, the fill factor depends on the temperature and it decreases with increasing temperature. The decrease in the FF is mainly controlled by a decrease in the V_{oc}, whereas the increase in I_{sc} with temperature does not give much to the fill factor.

1.4.6 Power Conversion Efficiency (*PCE*)

It is an important factor in comparing the characteristics and performance of one solar cell to another. The power conversion efficiency (PCE) is the ratio of energy output (P_{max}) from the solar cell to input energy (P_{in}) from the sun.

$$PCE\ (\eta) = \frac{V_m I_m}{P_{in}} \times 100\% \quad (1.5)$$

Efficiency is connected to I_{sc} and V_{oc}. Using equation (1.4) and equation (1.5),

$$\eta = \frac{V_{oc} I_{sc}}{P_{in}} \times FF \quad (1.6)$$

In addition, the efficiency of the solar cell influences the temperature, spectrum, and intensity of the incident sunlight. Therefore, the situation in which the efficiency is measured for performance comparison must be carefully controlled [20]. The performance of the solar cells

is calculated using the AM 1.5 G (air mass) standard. Here, the air mass is the amount through which solar radiation travels and is interrelated to the amount of absorption (AM= $1/\cos\theta$), where θ is the angle of the sun to the verticals. The AM 1.5 G is a standardized version of this spectral irradiation (with an integrated power density of 1000 W/m^2, $\theta = 45^o$) [21].

1.5 Generations of Solar Cell

Solar cells are categorized as the first, second, and third generations.

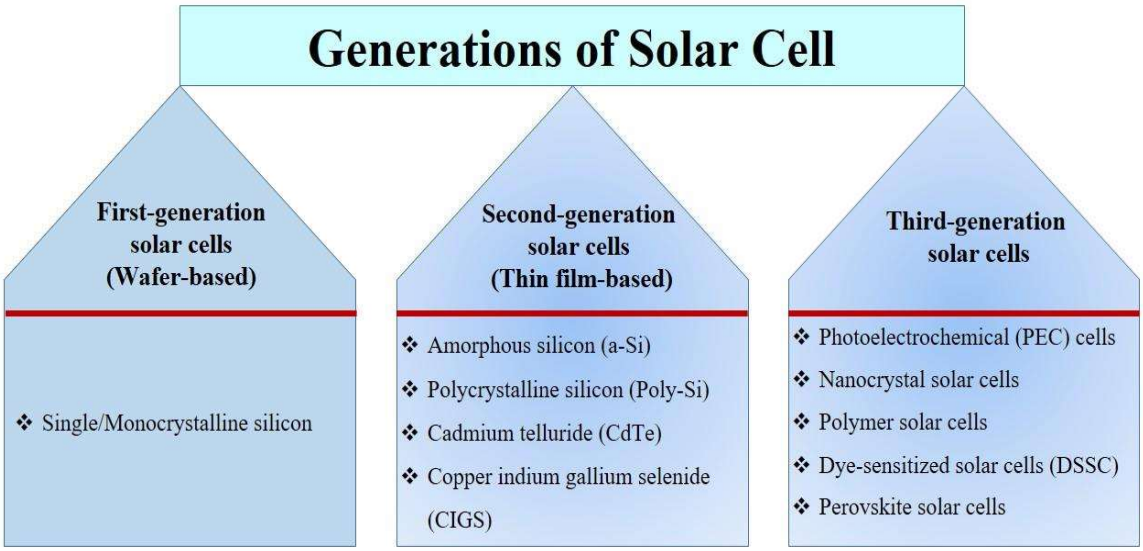

Figure 1.8: Represents the generations of the solar cell [22].

The first generation solar cell is the single-junction cells based on wafers built from single crystals or polycrystals for the PV technologies. The p-n junction based on amorphous Silicon semiconductor, which provided an efficiency of 6% at Bell Laboratories in 1954, began to attract widespread attention and the first generation photovoltaic technology is considered to consist of PV technology based on thick crystalline films (mainly Si), leading to not only high efficiency but also high cost [23]. Silicon-based solar cells currently dominate the PV market

by achieving high efficiencies of over twenty-six percent in parallel with the "modest" fabrication cost. But the disadvantage of silicon-based solar cells is that it exhibits harsh preparation conditions and high cost. The second-generation solar cells based on the thin-film PV device are made of the amorphous silicon CIGS, and CdTe. III-V semiconductor-based thin-film technologies demonstrated good efficiencies. This technology is cheaper but the downside of the thin-film technology is the less power conversion efficiency (PCE) than the conventional crystalline silicon technology. Third-generation PV technology includes dye-sensitized solar cells (DSSCs), organic, quantum dot cells, polymer, and perovskite solar devices. In which the role of perovskite materials is gaining immense importance among researchers due to easy processing conditions, excellent PV performance, and low-cost raw materials. Since the present research work is based on the perovskite solar cells. Therefore, it is important to understand what are perovskite and its different forms.

1.6 Perovskite (3D and 2D) Crystal Structure: An Overview

The crystal structure of perovskite is similar to the mineral with the chemical formula of $CaTiO_3$ (Calcium titanium oxide). *Gustav Rose* first discovered this mineral in 1839 in the Ural Mountains of Russia and name it after Russian mineralogist *L. A. Perovski*. The same crystal structure is present in materials with the general chemical formula of AMX_3, where M and A are cations with different ionic radii in which 'M' atoms are smaller than the 'A' atoms, while X represents an anion. The ideal perovskite structure (AMX_3) is a cubic cell having M cation in 6- fold coordination, surrounded by an octahedron of anions (X), and the A at the corner positioned of the cubic cell in 12- fold cuboctahedral coordination (Fig. 1.9) [24], [25]. For the halide-based perovskites, X anion can be Chlorine (Cl), Bromine (Br), or Iodine (I). M cation care Lead (Pb^{2+}), Germanium (Ge^{2+}) or Tin (Sn^{2+}), and A cations can be Cesium (Cs^{+}), FA

(formamidinium NH_2CH = NH_3^+), MA^+ (methylammonium, $CH_3NH_3^+$), EA (ethylammonium, $CH_3CH_2NH_3^+$), or Rubidium (Rb^+) [26]. The relative ion size is very important for maintaining the stability of the crystal structure in the perovskite cubic structure. Thus, a small change in the ion size will cause a distortion in the structure. *Victor G. Goldschmidt* developed the Goldschmidt tolerance factor as a good tool to examine the distortions and crystal structure stability [27].

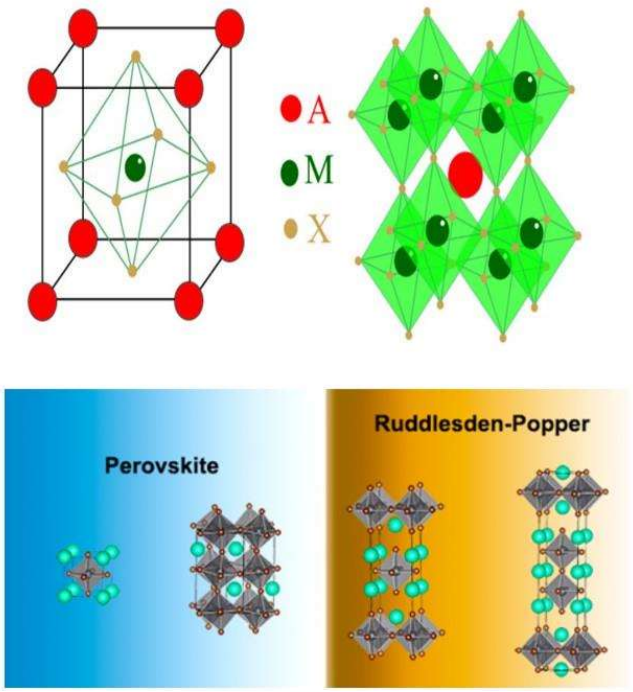

Figure 1.9: Represents the crystal structure of the perovskite and Ruddlesden-Popper materials [28].

Here, the Goldschmidt tolerance factor is abbreviated as τ, as described by the equation:

$$\tau = \frac{(r_A + r_X)}{\sqrt{2}\,(r_M + r_X)} \qquad (1.7)$$

Where, r_X, r_M, and r_A, represent the ionic radii. For an ideal cubic perovskite structure, the tolerance factor is equal to 1. The tolerance factor can be also modified by changing the ionic radii ions. The ratio of $\mu = R_M/R_X$ is the octahedral factor. The value of τ and μ should be, $0.81 < \tau < 1.11$ and $0.44 < \mu < 0.90$ to achieve stable halide perovskite [29]. If τ is lower, it forms less symmetry such as tetragonal or orthorhombic perovskite. In the case of $\tau > 1$, it destabilized the 3D (three-dimensional) M-X framework which lead to a 2D layered structure. μ is directly related to the octahedral structure. If $\mu > 1$, we observe MX_6 octahedral in a stable form and destabilize MX_6 octahedral form for the lower μ value. In perovskite materials, a tolerance factor is a good tool for identifying comparisons with empirical results. When we change the elements in the structure or mix perovskite. At that point, we can investigate which ions or elements would be too large or small to fit into the perovskite structure.

In addition, Ruddelesden–Popper (RP) perovskites (2D) have attained widespread importance as candidates for next-generation optoelectronic devices. Because of their stronger quantum confinement effect, better stability to moisture, and larger exciton binding energy than 3D perovskite [30].

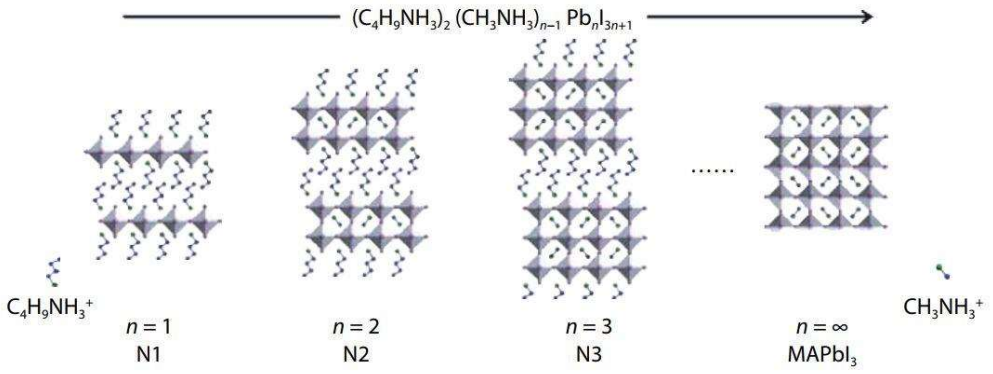

Figure 1.10: Depicts the Ruddlesden-Popper (RP) perovskite crystal structure with increasing 'n' values [31].

The RP perovskite structure employs a layer structure mixed in periodic patterns with 2D and 3D structures. The Ruddlesden-Popper chemical formula is $A_{n+1}M_nX_{3n+1}$; here denotes the distance between the 2D layers. If n = 1 then this represents one (1) layer of 3D perovskite between each 2D layer. A pure 3D perovskite solar cell has n = ∞. It consists of indefinite layers of three-dimension perovskite that do not have two-dimension perovskite layers (Figure 1.7) [32],[33]. Furthermore, the hydrophobic nature of the Rudelsden–Popper (2D) perovskite, the layered structure produces natural quantum wells that show greater insulating behavior [34]. Therefore, RP perovskites have tunable bandgaps with manipulation of their 'n' value. The bandgap of the material is larger with a lower 'n' value.

1.7 Perovskite Solar Cells

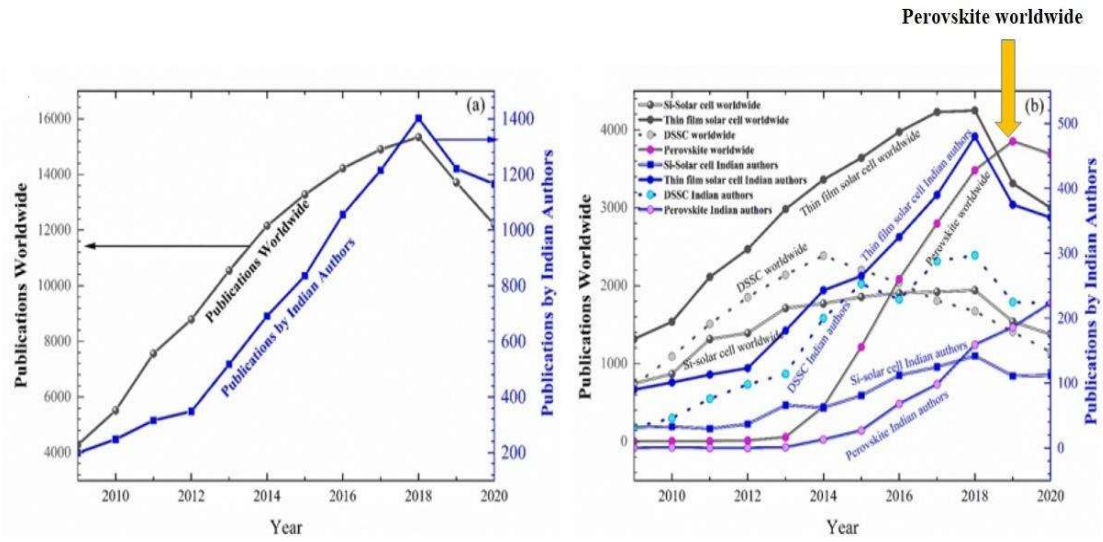

Figure 1.11: (a) and (b) represents year-wise publications worldwide and publications by Indian authors [35].

Fig. (1.11(a) and (b)) shows the year-wise publication pattern on solar cells, in which the left-hand side is the publication worldwide and the right-hand is the publication by Indian authors. This publication trend from 2010 to 2020 (Year-wise) indicates that the scope of research in the field of perovskite solar cells has grown faster than other technologies. Fig. 1.12 shows the power conversion efficiency of PSCs with other technologies. Moreover, this graph represents that the power conversion efficiency of other technologies other than perovskite solar cells from 1975 has been increased slowly. But within thirteen years (2009 to 2022), Perovskite is showing excellent efficiency compared to other technology (Fig. 1.12, shown in circle). Currently, perovskites are of excellent research interest as they have achieved a power conversion efficiency of more than 25% (Fig. 1.12). Astonishingly, in such a short time the power conversion efficiency has come so fast that it is approaching other technologies (thin film and silicon (Si)). It became even more impressive to see these results. For the past several years, researchers are exploring low-cost device structures with excellent efficiency and new materials to demonstrate PV effects. Perovskite solar cell (PSCs) having perovskite AMX_3 structure (A= Cs^+, MA= $CH_3NH_3^+$, FA= HC $(NH_2)_2^+$; M=Pb^{2+}, Sn^{2+}, Mn^{2+}; X= I, Br, Cl) where, X is the anion. M and A represents the cations [36]. Which has been found to show excellent properties in the field of solar cells. In addition, there are several reasons why perovskite solar cells are highly efficient and are of great interest to the community. These materials have been used as active material because of long charge carrier lifetime, high optical absorption (~10^5 cm^{-1}), the low exciton binding energy (~10 meV, long carrier diffusion lengths (>1 μm), high open-circuit voltage, the band gap (1.2 to 3.0 eV) can be adjusted (mixed halide (X= Cl, Br, I) perovskites), charge carrier mobility (~10 cm^2 V^{-1} s^{-1}), and low-cost fabrication [37],[38],[39].

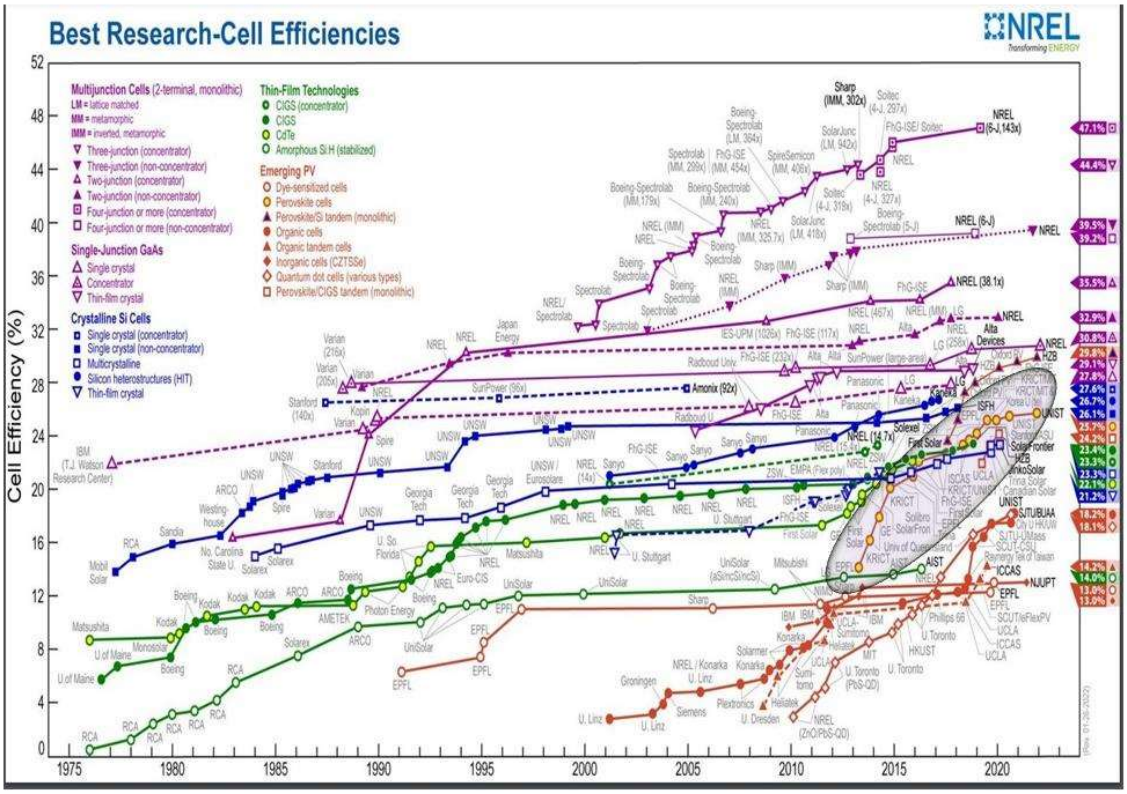

Figure 1.12: Power conversion efficiency trend with different technologies from NREL map [40].

It is discussed above, PCE of organic-inorganic hybrid PSCs achieved above 25% However, the issue of material degradation and the current-voltage hysteresis problem exists. Therefore, this problem must be addressed first before commercializing can be used. There are two major problems in the perovskite solar cells. First is the stability issues and the second is the I-V hysteresis.

1.7.1 Stability Issues

In the past few years, organic-inorganic/mixed halide hybrid perovskites have shown up as the most promising photovoltaic materials. However, organic-inorganic halide perovskites suffer from thermal instability due to the instability of organic cations in perovskite compositions [41],[42]. Moreover, the thermal degradation and photodecomposition processes

of methylammonium lead iodide ($MAPbI_3$) lead to irreversible decomposition to (CH_3I + NH_3), reversible generation of I_2, (CH_3NH_2 + HI, reversible decomposition), mild heat conditions or non-volatile Pb^0 under illumination and one arrow sign represent the irreversibility of the process of releasing CH_3I + NH_3 for the reaction (Fig 1.13(a)) [43],[44],[45]. In addition, the perovskite materials are promising compounds for photodetectors, light-emitting diode (LED), and lasers despite the environmental degradation caused by humidity and heat [46],[47],[48]. These perovskite materials have proven to be effective for solar cell devices with excellent efficiency. However, this technology currently exhibits a stability problem and low power conversion efficiency. Furthermore, extrinsic and intrinsic factors are two issues that affect the stability loss or degradation of the devices. Heat, oxygen, exposure, and moisture are extrinsic factors and these factors degrade the PCE of devices (Fig. 1.13(b)) [49]. The extrinsic factor can be prevented through passivation or encapsulation schemes of the perovskite layer [50],[51]. However, the intrinsic factor is the more problematic nature for the degradation. Defects such as ion interstitials and ion vacancies can easily arise in the perovskite lattice [52]. It has been reported that in organic-inorganic halide perovskites, ion migration leads to the current hysteresis behavior in PSCs, which is dominated by the grain boundary in perovskite films [53],[54]. The migration of ionic species (or charge defects) in perovskite materials remains a major concern as to whether these materials can retain their optoelectronic properties during harsh and prolonged operating conditions [55]. Moreover, Cs atoms doped in perovskite solar cells have been increased the stability of materials and the efficiency of a solar cell [56]. In inorganic perovskite halides, the phase control of $CsPbI_3$ material is complicated in the air at room temperature.

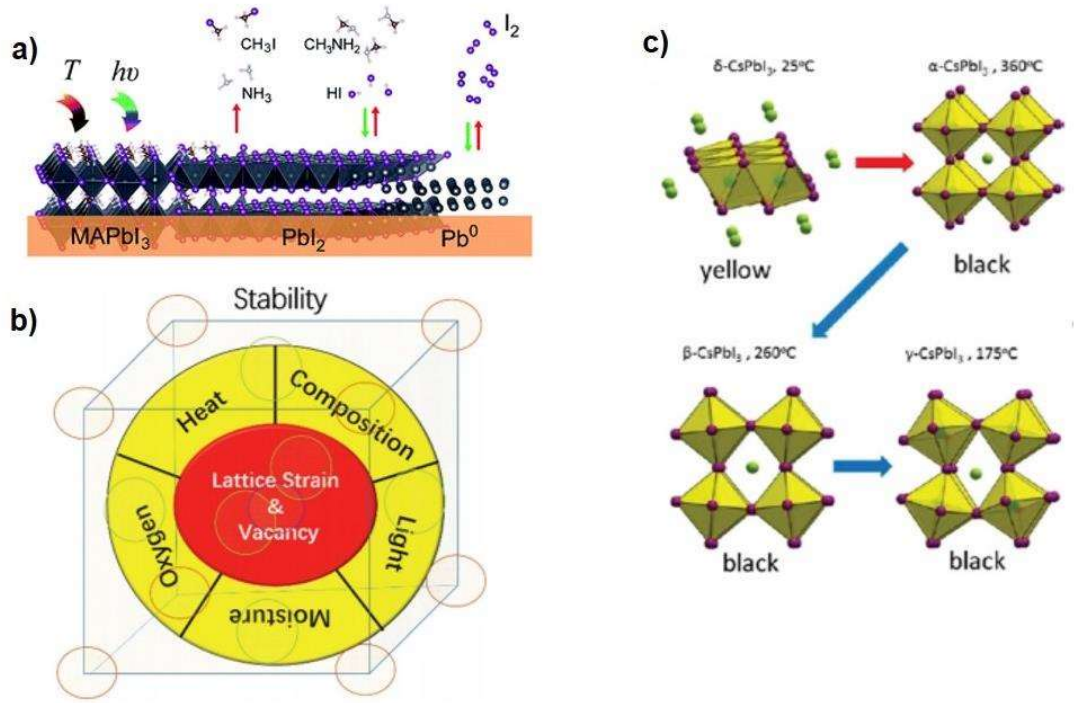

Figure 1.13: (a) Represents photodecomposition and thermal degradation processes of $MAPbI_3$. (b) Extrinsic and intrinsic factors (c) $CsPbI_3$ phases [57],[36].

$CsPbI_3$ is reported to have four phases: cubic (α-phase), tetragonal (β-phase), non-perovskite yellow orthorhombic phase (δ-$CsPbI_3$) and perovskite black phase (γ- $CsPbI_3$) (Fig 1.11(c)) [58]. However, this phase converts into the orthorhombic phase at room temperature [59]. Therefore, $CsPbI_3$ material has been studied by many researchers because of its low bandgap [60],[61]. Furthermore, the thin film of $CsPbI_3$ is not stable despite the bandgap narrowing [62]. However, the thermal stability of PSCs can be improved by the doping of cesium (Cs) instead of organic cations [63]. Many of the researchers are focusing on the synthesis and reducing the bandgap of cesium lead halides after dopping on A, B, and X sites [64],[65],[66].

1.7.2 Current-Voltage (I-V) Hysteresis

Despite the promising features for future photovoltaic applications for perovskite halides, current-voltage hysteresis remains the biggest puzzle to be solved before industrialization. All possible causes ranging from classical (ie, slow transient capacitance, morphology, defects, etc.) to quantum (ie, spin-orbit interactions) are investigated. However, its origin is still debated, as the possibilities have shown some ambiguity over the science so far known. As discussed above, the recent increase in perovskite materials (ABX_3) for high-efficiency and low-cost solutions for solar cells has attracted researchers from almost all corners of the science and technology communities [67],[68],[69]. Thanks to a decade of intensive research on these organo-inorganic halides, a significant increase in solar efficiency from 4% (2009) to 25.5% (2021) have been observed [70],[40]. Although the stability of these samples is still a matter of concern, rapid progress is being seen in this direction as well [71]. It is also observed that both mixed ($CH_3NH_3PbI_3$) and all inorganic ($CsPbI_3$ and $CsPbBr_3$) perovskite halides are intrinsically stable as suggested by their thermal analysis [72],[73]. However, extrinsic factors such as electric field, heat, moisture, etc. do not allow ($CH_3NH_3PbI_3$) to last long; However, all inorganic perovskites are quite stable (structurally) in their bulk form, although the stability (photo-stability) of perovskite halides under light is also a major issue that has not been extensively investigated [74],[75],[76]. Furthermore, the photo-instability of perovskite halides is in correlation with the problem of current-voltage hysteresis, which needs to be addressed to estimate the true photon to electron efficiency.

The hysteresis problem in perovskite was first reported in 2014 [77],[78]. This hysteresis complicates and challenges the estimation of the efficiency (energy storage density) of perovskite solar cells (PSCs) designed in various structures. Since then, some hypotheses have been proposed

[79],[80]. It depends on several parameters such as scan rate [77], applied voltage [81], scan direction [82], preconditions, and architecture [83],[84]. Several reports are available regarding the mechanism of hysteresis and it has been claimed that the hysteresis behavior arises due to slow transient capacitive current [85], trapping–de-trapping process [86], band bending due to ion migration [87],[88], and band bending due to ferroelectric polarization [89]. The Rashba effect (momentum-dependent splitting due to symmetry breakage) has also been reported to cause hysteresis in PSCs [90]. Furthermore, ferroelectricity is unable to explain the non-steady current (hysteresis) [91]. Short circuit current density (J_{SC}), revealed the voltage dependence and slow decay characteristics of hysteresis [92]. It is also speculated that the hysteresis is mainly due to capacitive current [85]. In addition, a high defect density is also reported to contribute to hysteresis and photo-degradation [93]. However, charge traps at the grain boundary and the surface of thin films are reported to eliminate hysteresis as it affects charge trapping on the electron/hole extraction efficiency [94]. Ion migration accumulates charge at the interface, causing band bending and a non-steady current with field [95],[96].

The partial or complete substitution of volatile organic cations (such as MA ($CH_3NH_3^+$), FA (HC $(NH_2)_2^+$) has been proven to overcome this problem, making it an effective method for improving device stability. The $CsPbX_3$ (X=Cl, Br, I) has been considered as an alternative because it has excellent optoelectronics properties and stability [97]. Cs-based all-inorganic hybrid perovskite has shown an enormous scope in photovoltaics. Among these perovskite materials, $CsPbBr_3$ is a promising candidate because of their optoelectronic properties [98].

1.8 Comparison of Cesium Lead Bromide ($CsPbBr_3$) Material with the Hybrid and All-Inorganic Perovskite Materials

It has been discussed above, organic perovskite materials are degraded rapidly under the ambient atmosphere. Loredana Protesescu et al. reported monodisperse colloidal nanocubes (4−15 nm edge lengths) of fully inorganic cesium lead halide perovskites ($CsPbX_3$, X = Cl, Br, and I or mixed halide systems Cl/Br and Br/I) using inexpensive commercial precursors. Through compositional modulations and quantum size-effects, the bandgap energies and emission spectra are readily tunable over the entire visible spectral region of 410−700 nm [99]. Moreover, presented fast, low-temperature, deliberately partial, or complete anion exchange in highly luminescent semiconductor nanocrystals of cesium lead halide perovskites ($CsPbX_3$, X = Cl, Br, I) [100]. Bo Li et al. presented highperformance and stable HTL free perovskite solar cells based on $MAPbI_3$- $CsPbI_{3-x}Br_x$ GHJ architecture is fabricated and characterized for the first time, which achieves a significantly enhanced PCE of 11.33% (nearly 40% increase compared with 8.16% for pure HTL free devices). Jin Hyuck Heo et al. demonstrated a monolithically integrated perovskite sub-module based on the graded $CsPbI_{3-x}Br_x$ by spray coating with an efficiency of 13.82% (112-cm^2 aperture area) and ~ 9% degradation over 1,000-h continuous 1-sun light soaking. Zhenzhen Li et al. reported the CsBr-Induced Stable $CsPbI_{3-x}Br_x$ (x < 1) Perovskite Films at Low Temperature for Highly Efficient Planar Heterojunction Solar Cells. In which, 0.5-CsBr film-based solar cells demonstrated a PCE of 10.92%, which shows the excellent PCEs of $CsPbI_{3-x}Br_x$-based solar cells. Also, the PCE of the optimal device could maintain its initial value for at least 192 h. As cesium lead halide ($CsPbX_3$) perovskites with rich Br content are structurally more stable. In 2015, Cesium lead

bromide ($CsPbBr_3$) PSCs has been first demonstrated by Kulbak et al. using a two-step sequential deposition method [101]. $MAPbI_3$ and $CsPbI_3$ perovskite materials are highly efficient but these materials have low stability as compared to the $CsPbBr_3$ sample in ambient conditions [102]. In addition, controlling the bandgap and phase stability of cesium lead iodide and methylammonium lead iodide perovskite materials is a challenging task for the researcher. The larger ionic radii of iodine (I^-) than that of bromide (Br^-) influence the phase stability under the ambient environment [103]. The phase stability can be improved by the increase of Br contents (as shown in Fig 1.14(a) and (b)). The cesium lead bromide device has superior stability as compared to the other devices in Fig. 1.14(c). Moreover, other inorganic thin films degrade rapidly in the ambient atmosphere (Fig. 1.14(d)). It has been reported by Akbulatov's group, cesium lead bromide $CsPbBr_3$ has excellent photostability as compared with methylammonium lead iodide ($MAPbI_3$) under illumination (Fig. 1.14(e)). The relative absorbance vs aging time with the different halide perovskite in which the cesium lead bromide sample exhibits superior stability as compared to other perovskite halides (depicts in Fig. 14(f)). Furthermore, most of the research work has been done on the lead-free perovskite halides to reduce the toxicity and good optoelectronics properties. Tin (Sn) has been considered as less toxic and has a smaller bandgap (1.2 to 1.8 eV) as compared to lead-based perovskite halides [104].

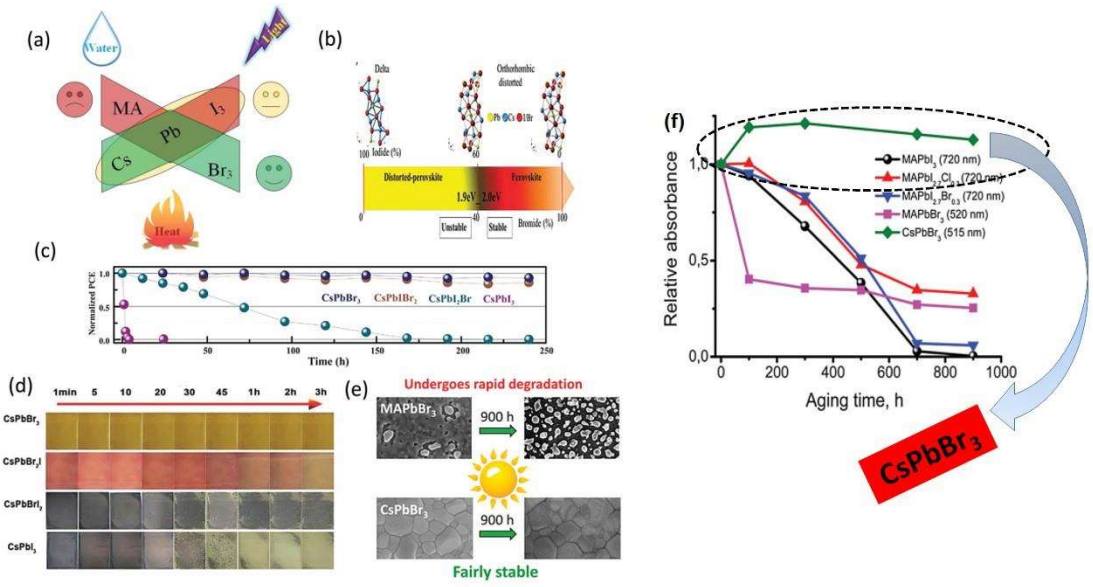

Figure 1.14: (a) The stability of the perovskites by the surrounding condition with the crystal structure of the perovskites (Fig.(b)). (c) Normalized PCE vs Time (h) spectra for perovskite solar cell devices. (d) Degradation of $CsPbI_{3-x}Br_x$ thin films exposed to ambient condition (e) Photo-stability of $CsPbBr_3$ and $MAPbBr_3$ perovskites. (f) Depicts the relative absorbance vs aging time [103],[105],[106],[107].

Therefore, tin-based perovskite has shown the following performance in photovoltaic applications and optoelectronic devices. But the disadvantage in tin-based PSCs, Sn^{2+} is easily oxidized to Sn^{4+} in the tin-based perovskite films which leads to high-density p-type doping [108]. Oxidized perovskite layers have a high nonradiative carrier recombination rate and a short carrier lifetime which influence the photovoltaic performance of the PSCs. Fig. 1.15(a) shows the PCE of the inorganic, organic, and Sn-Pb mixed perovskite solar cells (PSCs). Pb-Sn mixed perovskites are becoming increasingly popular as narrow-bandgap (1.2–1.3 eV) light absorbers in single-junction perovskite solar cells (PSCs) and as bottom cells for all-perovskite tandem solar cells, for high-efficiency, lightweight, low-cost, roll-to-roll printable photovoltaic (PV) applications. The inorganic perovskite is more stable with minimum

efficiency than that of the organic perovskite. Therefore, many researchers have been working to increase the PCE of the PSCs by mixing the organic and inorganic perovskite.

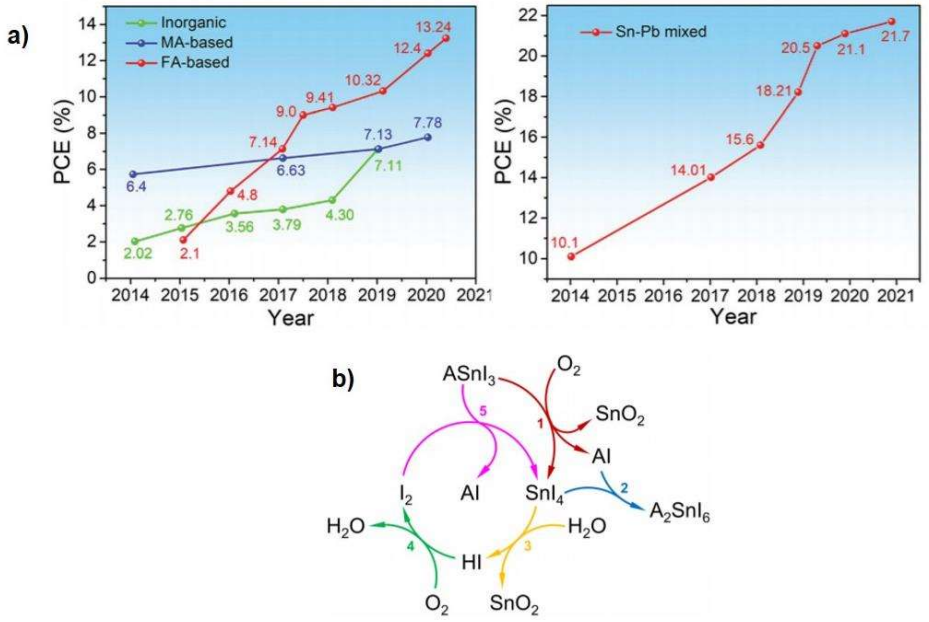

Figure 1.15: (a) Represents the power conversion efficiency of tin (Sn)-based with organic and Sn-Pb mixed perovskite solar cells. (b) Cyclic degradation mechanism of tin iodide (SnI_4) in ambient condition [109],[110].

Moreover, tin (Sn) is also used with lead (Pb) to increase the PCE. The PCE of the PSCs has been achieved above 21% by mixing Sn-Pb in Fig 1.15(a). The mixing of Sn with Pb shows superior stability as compared to pure tin-based perovskite halides. Fig. 1.15(b) shows the cyclic degradation mechanism in ambient conditions. It has been reported that in Fig 1.15(a), A is the organic cations (prepared of the hybrid tin perovskite, 20% PEA and 80% A=FA). Reaction 1 is showing the oxidation of perovskite by oxygen (O_2) with the formation of tin iodide (SnI_4); reaction 2, SnI_4, and AI converted into the solid-state formation of $ASnI_6$. Reaction 3 shows the hydrolysis of tin iodide (SnI_4) by HI and H_2O formation. Reaction 4,

converts I_2 formation because of oxidation of HI by O_2. Finally, converted into the tin iodide (SnI_4) formation due to the oxidation of perovskite by I_2.

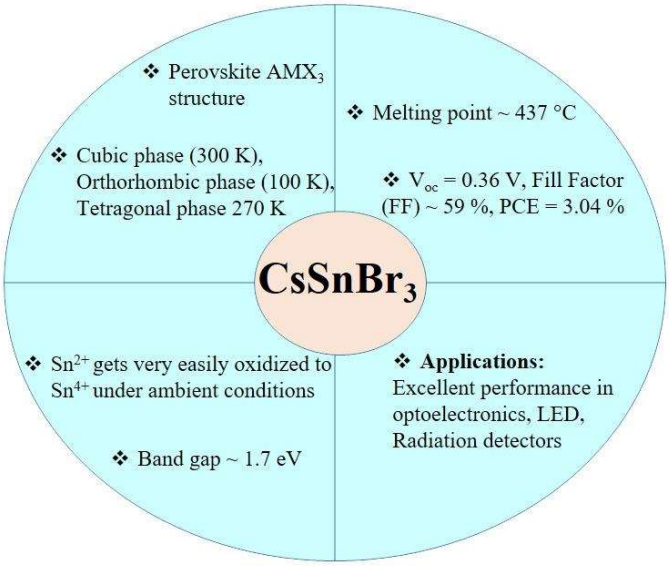

Figure 1.16: Overview of $CsSnBr_3$ perovskite material properties [111],[112].

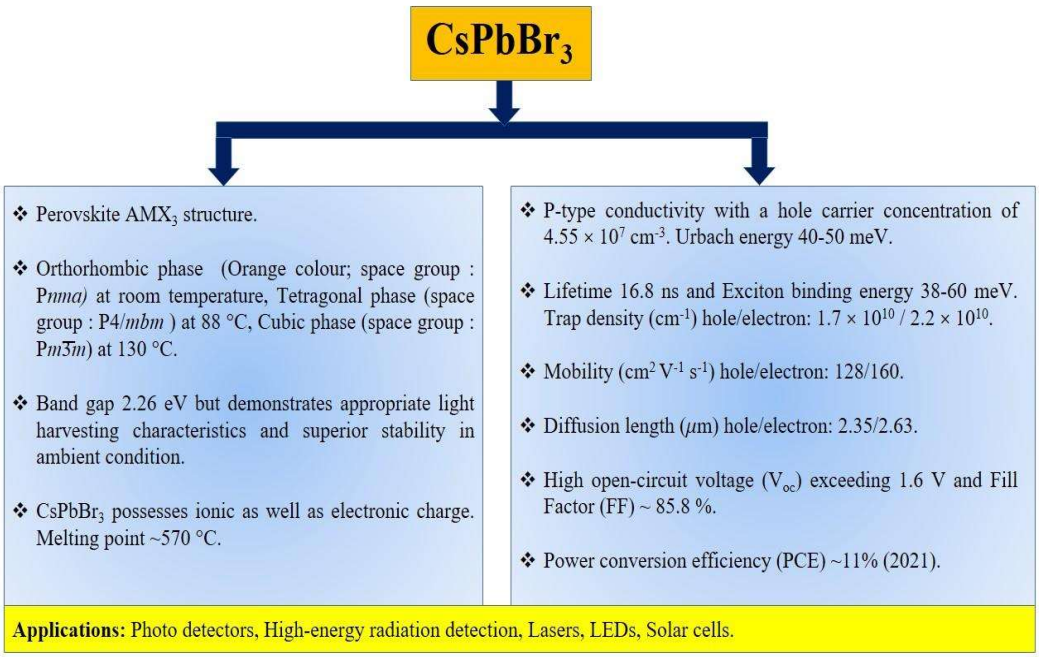

Figure 1.17: Overview of $CsPbBr_3$ perovskite material properties [107],[113],[114],[115],[116].

It is concluded that cesium lead bromide ($CsPbBr_3$) has superior phase stability, photostability, and stable absorption among all perovskite halides. Although a vast amount of literature is available, this area is still emerging. It needs investigating and understanding the stability and current-voltage hysteresis problem for the application of solar cells.

1.9 The objective of current research

It is also discussed that the major problem of stability issues and I-V hysteresis for perovskite halides are discussed earlier in this chapter. Therefore, the main objective of the current research work is to try to address stability issues and investigate current-voltage (I-V) hysteresis in perovskite halides. It is essential to understand the problem of current-voltage hysteresis and stability with the synthesis process, which must be solved before industrialization for photovoltaic applications.

There are some points to solve the problem of hysteresis, such as

(a) Band bending.

(b) How the interfacial photo-electron/hole with the trapped charge and mobile ions affects the capacitive current.

(c) The interaction between ion migration and electrode polarization.

(d) The time scale required for redistribution of mobile ions.

For this purpose, Inorganic perovskite $CsPbI_3$, $CsPbBr_3$, and their Ruddlesden Popper (RP) Cs_2PbBr_4, Cs_2SnBr_4 have been selected as active layer materials. For the ETL and HTL,

TiO_2 and CuO materials have been selected, respectively. The precise objectives of the thesis work are as follows:

1. To address the stability issues and understand the degradation mechanism, active materials $CsPbI_{3-x}Br_x$ (x=0.0 to 3.0, in the step size of 0.5) series are synthesized by the solid-state reaction route via cold sintering method in the air at room temperature and studied the physical properties.
2. Time-dependent photoconduction studied of $CsPbBr_3$ Perovskite to investigate the current-voltage hysteresis.
3. Comparative studies of $CsPbBr_3$ and $CsSnBr_3$ Perovskite and Cs_2PbBr_4 and Cs_2SnBr_4 Ruddlesden- Popper (RP) halides.
4. In addition to the physical properties of compounds, ion dynamics investigations of some compounds at elevated temperatures.
5. Study the photostability of Perovskite $CsPbBr_3$ and $CsSnBr_3$ thin films and devices using the Pulsed Laser Deposition (PLD) technique.
6. Study the Interfacial absorption behavior ETL/Perovskite and HTL/Perovskite by theoretical simulation using Finite Element Method (FEM). Through FEM simulation, $TiO_2/CsSnBr_3$ showed absorbance ~80% for 200 nm thickness. While $TiO_2/CsPbBr_3$ with 700 nm thickness has shown ~100% absorbance (This might be the reason for higher current). At $CuO/CsPbBr_3$ and $CuO/CsSnBr_3$ interface, both have the same absorbance but electric field distribution is different. ETL/perovskite plays a role in the I_{sc} rather than HTL/perovskite interface. This theoretical study will help to understand the interfaces such as ETL/perovskite and HTL/perovskite problems.

Description of the synthesis process and measurement techniques for the compounds investigated are described in the next chapter.